Tone and call responses of units in the auditory nerve and dorsal medullary nucleus of *Xenopus laevis*

Taffeta M. Elliott,
Neurobiology and Behavior, Columbia University, New York, NY, USA. UC Berkeley, Helen Wills Neuroscience Institute, 3210 Tolman Hall, Berkeley, CA 94720, USA

Jakob Christensen-Dalsgaard, and
Institute of Biology, University of Southern Denmark, Odense, Denmark

Darcy B. Kelley
Neurobiology and Behavior, Columbia University, New York, NY, USA. Biological Sciences, Columbia University, New York, NY, USA

Taffeta M. Elliott: taffeta@berkeley.edu

Abstract

The clawed frog *Xenopus laevis* produces vocalizations consisting of distinct patterns of clicks. This study provides the first description of spontaneous, pure-tone and communication-signal evoked discharge properties of auditory nerve (n.VIII) fibers and dorsal medullary nucleus (DMN) cells in an obligatorily aquatic anuran. Responses of 297 n.VIII and 253 DMN units are analyzed for spontaneous rates (SR), frequency tuning, rate-intensity functions, and firing rate adaptation, with a view to how these basic characteristics shape responses to recorded call stimuli. Response properties generally resemble those in partially terrestrial anurans. Broad tuning exists across characteristic frequencies (CFs). Threshold minima are −101 dB re 1 mm/s at 675 Hz; −87 dB at 1,600 Hz; and −61 dB at 3,000 Hz (−90, −77, and −44 dB re 1 Pa, respectively), paralleling the peak frequency of vocalizations at 1.2–1.6 kHz with ~500 Hz in 3 dB bandwidth. SRs range from 0 to 80 (n.VIII) and 0 to 73 spikes/s (DMN). Nerve and DMN units of all CFs follow click rates in natural calls, 67 clicks/s and faster. Units encode clicks with a single spike, double spikes, or bursts. Spike times correlate closely with click envelopes. No temporal filtering for communicative click rates occurs in either n.VIII or the DMN.

Keywords

Auditory nerve; Hearing; Amphibian; Dorsal medullary nucleus; Sound communication

Introduction

The South African clawed frog, *Xenopus laevis*, communicates underwater at night using a rich vocal repertoire (Kelley and Tobias 1999). Call types consist of trills produced with distinctive patterns of click rates, and evoke very different responses from conspecifics. For example, the female call rapping, a fertility call that precedes oviposition, is composed of rapid (13 Hz) clicks and stimulates male advertisement calling and answer calls (Tobias et al. 1998). In contrast, ticking, a call made by sexually unreceptive females in response to a

Correspondence to: Taffeta M. Elliott, `taffeta@berkeley.edu`.

clasping male, is composed of slower (4 Hz) clicks and suppresses male advertisement. If clicks taken from ticking calls are presented at the rapping click rate, males respond with invigorated calling as they would to natural rapping (Elliott and Kelley 2007). The stimulating effect of rapping relies primarily on temporal rather than spectral features or click amplitude (Vignal and Kelley 2007). Temporal characteristics of calls are also important in male–male interactions. The male advertisement call, for example, alternates between slow and fast trills and suppresses calling in neighboring males. The advertisement call differs from the male answer call (which is not commonly suppressive in male–male interactions) in the relative duration of the slow and fast trills and in the between-click amplitude modulation of the fast trill (Tobias et al. 2004). The ability of the auditory system to respond differentially to different click rates and temporal patterns is essential for appropriate behavioral responses.

Xenopus arose from terrestrial ancestors 70–80 Ma (Trueb 1996; Evans et al. 2004). Features of the auditory system may reflect the evolutionary adaptation of this genus to sound transmission and reception in aquatic habitats. *Xenopus* clicks are somewhat briefer (<5 ms) and therefore, more broadband (500 Hz bandwidth at half amplitude) than the amplitude-modulated pulses produced by the vocal cords of Ranidae, Hylidae, and *Physalaemus pustulosus* (Gerhardt and Huber 2002). The temporal distinctiveness of click rate, and the dominant energy peak within each click at 1.2 or 1.6–1.8 kHz (high relative to frogs of comparable size; Gerhardt and Schwartz 2001), could be indicative of a communication signal evolutionarily selected for invariance under high-pass frequency filtering in the shallow underwater habitat where wild *Xenopus* produce and listen to calls (Yager 1992).

Hearing in *Xenopus* is also adapted to the aquatic environment (Yager 1992; Elepfandt 1996). Instead of an eardrum *Xenopus* has a cartilaginous tympanic disk, beneath the skin posterolateral to the eye, that vibrates like a plate in response to underwater sound. The vibration of the tympanum is enhanced by resonances of enclosed air in the middle ear cavities (Christensen-Dalsgaard and Elepfandt 1995). Underwater sound impinging on air-filled cavities inside the middle ear normally drives the tympanum from within. Acoustic energy is transferred from the tympanum to the oval window by the columella (Wever 1985). Two inner ear organs, the amphibian and basilar papillae (AP and BP), transduce the resulting fluid movement within the otic capsule. The papillae are innervated by fibers of the eighth nerve (n.VIII), whose cell bodies originate in the acoustic ganglion, and whose axons terminate on cells of the dorsal medullary nucleus (DMN) of the hindbrain (Capranica 1976; Lowe 1986). In *Xenopus*, the ratio of BP to AP fibers is 0.63, apparently larger than in terrestrial frogs (Will and Fritzsch 1988). Additionally within the inner ear, the saccule may contribute to detecting sound and lower-frequency vibrations (Christensen-Dalsgaard and Narins 1993).

To investigate the processing of acoustic information entering the *Xenopus* central auditory system, we recorded in vivo from n.VIII fibers and DMN neurons using pure tones and recorded calls as stimuli. The DMN is the first nucleus in the ascending auditory pathway, and an analogue to the cochlear nucleus in mammals. We characterized response patterns over time as a function of temporal and spectral acoustic features. In order to bypass the intricacies of underwater sound stimulation, we devised a method to deliver stimuli by direct vibration of the tympanic disk. Because the tympanic vibration velocity has been measured with laser vibrometry during underwater sound stimulation (Christensen-Dalsgaard and Elepfandt 1995), we can directly compare our stimulation to underwater sound delivery. This method has allowed us to begin an investigation of where temporal coding arises in the

Xenopus auditory system, and in particular, to relate neural activity to the acoustic parameters known to be behaviorally relevant in female and male calls.

Materials and methods

Animals and surgery

Adult male and female *Xenopus laevis* were obtained from Nasco (Ft. Atkinson, Wisconsin, USA), *Xenopus* One (Ann Arbor, Michigan, USA), and the August Krogh Institute of the University of Copenhagen in Denmark. Body weights were 20–94 g in males and 68–109 g in females. Frogs were maintained under a 12-h light/dark cycle at 17–22°C and fed frog brittle twice weekly (Nasco). Auditory nerve recordings were carried out in six males and six females, and DMN recordings in six males and three females.

Before surgery, frogs were anesthetized by injection of MS-222 (tricaine methanesulphonate, 2.6% at 10–20 μl/g b.w., Sigma-Aldrich, Brøndby, Denmark) into the dorsal lymph sac and placed on ice to maintain anesthesia. The skull medial to the otic capsule was thinned to expose the choroid plexus above the right n.VIII just lateral to the brainstem. A gelatin sponge (Spongostan, Ferrosan, Søborg, Denmark) packed the wound overnight. When the frog recovered, the skin edges and muscle surrounding the wound were treated with lidocaine (5%, AstraZeneca DD427, Albertslund, Denmark). The DMN was similarly exposed using a dorsal approach (Jørgensen and Christensen-Dalsgaard 1997), modified in that the adjacent brainstem (Paton et al. 1982) was further exposed, nearly to the midline, together with the auditory nerve.

On the morning of each neurophysiological recording day, we injected curare (D-turbocurarine chloride, 12 μg/g b.w.; Carl Roth, Karlsruhe, Germany) intramuscularly to paralyze the frog. Immobilization was maintained throughout the experiment by subsequent injections (150–300 μg) every few hours. In pilot experiments, frogs were also injected with Fentanyl (Haldid, Janssen, 1.4 nM/g; IACUC protocol AC-AAAA1277); however, additional study revealed that fentanyl has no analgesic or anesthetic effect in *Xenopus* (unlike in ranids; Bodnar and Capranica 1994; Stevens et al. 1994; Jørgensen and Christensen-Dalsgaard 1997) and this treatment was discontinued. Thus, frogs were anesthetized only locally during recordings. To confirm adequate oxygenation, we monitored blood flow on the brain and in the eye and stopped recording if circulation was poor. A regression performed on the acoustic threshold as a function of recording number in each individual revealed that sensitivity did not decline as the recording session progressed ($r = 0.04$, n.VIII; $r = 0.008$, DMN). The gelatin sponge was removed and the choroid plexus was retracted medially with a minuten pin hook, exposing n.VIII and part of the brainstem. The frog's skin was kept moist with dampened tissue throughout surgery and recording. Cutaneous O_2 accumulation measured in *Xenopus* in air is 10–16 $\mu l\, cm^{-2}\, h^{-1}$, providing respiration sufficient for resting metabolism (Bentley and Shield 1973). With its jaw supported by modeling clay, the animal lay dorsal-side up on a vibration exciter (4809, Brüel & Kjær, Nærum, Denmark) inside a sound-isolated Faraday cage, on top of a vibration-damped base. The vibration exciter vibrated the whole body so recordings of saccular fibers could be excluded (see below). Room temperature ranged seasonally from 17 to 20°C. Over this range there are no systematic effects of temperature on auditory thresholds or frequency selectivity. Stimuli, electrode movements, and data acquisition were controlled from an adjoining room. Animals were overdosed with MS-222 and frozen at the end of the experiment.

Recording procedures

Extracellular single-cell activity was recorded using glass microelectrodes (20–40 MΩ). A piezo micromanipulator (PM-10, Märzhäuser, Wetzlar-Steindorf, Germany) advanced the electrode in steps <10 μm. After amplification (Cyto721, World Precision Instruments, Sarasota, FL), the electrode signal was fed to a real time spike discriminator and event timer (Tucker Davis Technologies—TDT system 2, SD1 and ET1, Alachua, FL, USA) for spike identification, sorting, and time logging (± 1 μs). In some cases, the electrode signal from the amplifier was recorded by an A/D converter (TDT AD2, system 2, 16 bit). Data recording and stimulus generation were controlled by custom-made software (FrogMaster 2-TV). Recording signals were monitored concurrently on an oscilloscope (PM3370 Fluke).

Electrodes were first positioned under low magnification according to contour landmarks on the brain surface. Auditory nerve recordings were obtained from a portion <0.5 mm from the lateral brain edge, outside the otic capsule. To record from the DMN, we positioned electrodes using the anatomical mapping of the nucleus by retrograde transport of a tracer from its target in the torus semicircularis (TS), identified in comparison with the corresponding Nissl-stained section (Edwards and Kelley 2001). In horizontal section, the DMN appears coextensive, anterior to posterior, with the posterior branch of n.VIII. In practice, the electrode was placed within the medulla from the most rostral level of n.VIII to 500 μm caudally. The DMN extends from a region just medial to the nerve insertion and as far as the mediolateral midpoint. In transverse section, the DMN extends 500 μm below the dorsal hindbrain surface. Auditory responses were routinely recorded from this operationally defined region and these recordings will be referred to as DMN recordings throughout the paper. Lateral line afferents are located much more medially and ventrally. Vestibular afferents were excluded experimentally as follows. The semicircular canals do not respond to frequencies above a few Hz. Saccular fibers or neurons in the nucleus saccularis were identified physiologically by low-frequency sensitivity (<100 Hz), together with thresholds to tympanic vibration that were at least 25 dB higher than thresholds to whole-body dorsoventral vibration, and excluded from analysis (Christensen-Dalsgaard and Narins 1993). Recording sessions lasted 8–17 h, and individual single units were held for up to 30 min.

Controlled vibration of the tympanum

We directly controlled tympanic vibration by attaching a custom-made vibration-exciter probe (4810, Brüel & Kjær) to the cartilaginous tympanum (Fig. 1c), since previous studies have measured large vibrations of the tympanic disk in response to underwater sound (Christensen-Dalsgaard and Elepfandt 1995). The major source of vibrations entering the inner ear is via columellar transmission from the tympanum. In addition to underwater sound impinging on the tympanum, sound-induced lung vibrations are efficiently transmitted to the tympanum and reach the inner ear by tympanic vibration. Although some low-frequency sound may reach the inner ear by extratympanic means such as the body cavity, we elicited strong responses from n.VIII and DMN units to stimuli as low as 100 Hz delivered solely by vibrating the tympanum.

Skin and fat were cut away from the tympanum (under local anesthetic as above) and the vibration probe was attached with cyanoacrylate tissue glue (Histoacryl, Braun Melsungen, Germany; Fig. 1c). Care was taken not to allow glue to fall on the tympanic annulus, nor to tonically displace the tympanum. Tympanum velocity amplitude was equalized within 0.5 dB in the experimental frequency range (50–3,200 Hz) by dividing the signal sent to the vibration exciter by the transfer function between vibration exciter input and probe vibration velocity. Probe vibration velocity was measured at the beginning of each experiment by an

accelerometer (4500-A, Brüel & Kjær, amplified by charge amplifier 2635, Brüel & Kjær, used with a 40 dB voltage divider) at the base of the probe and recorded on the A/D converter.

Stimuli

Tympanic stimuli included trapezoidal pure tone pulses, and digitized underwater recordings of four *X. laevis* call types from the field and from laboratory tanks (Cornell Bioacoustics Program hydrophone, Ithaca, NY, output sensitivity -163 ± 3 dB at 1 V/μPa, frequency sensitivity 0.015–10 kHz; Marantz cassette tape recorder PMD430, 16 bit, sampled at 22.05 kHz, Fig. 1a). Small sections (8,000 points, i.e., 370 ms) of these calls were stored in order to test all cells with identical segments. The peak amplitude of call signals was normalized to be 0 dB re 1 mm/s. All stimuli were A/D converted (AD2, TDT), filtered, passed through digital attenuators (PA4, TDT; and 2125, Hatfield Instruments) and amplified through a custom-built, battery-driven 10× amplifier. Dorsoventral vibrations were generated similarly and calibrated by a Brüel & Kjær 4321 accelerometer placed next to the frog's head on the platform.

The four call types (Fig. 1a) differed in temporal characteristics: female ticking (4.3 Hz click rate), female rapping (14.5 Hz), the slow trill of the male advertisement call (33.3 Hz), and the fast trill of male advertisement (mean 46.9; 62.5 Hz at the fastest). The maximal energy in the spectral content of female clicks is at ~1.2 kHz, while energy in male clicks peaks at ~1.7 kHz (Fig. 1b).

Experimental protocol

Search stimuli consisted of tympanic frequency sweeps (60–3,200 Hz) and whole-body dorsoventral vibration sweeps (10–100 Hz). Click trains were presented whenever a unit failed to respond. No unit responded to only click trains. Units were isolated aurally by means of a loudspeaker broadcasting the recording signal and visually by means of the oscilloscope. When a unit was isolated, a series of 150 ms tone bursts (in 1/6 octave steps 100–3,200 Hz) was presented at an intensity preferably high above threshold (typically 15 to −60 dB re 1 mm/s) to roughly estimate frequency preference and sensitivity. The characteristic frequency (CF) was determined with an automated threshold tracking technique (adaptive staircase; Levitt 1971) using tones as high as 3,600 Hz. The criterion for threshold was a sound-induced spike rate 10% above the spontaneous activity taken over the preceding 2 s (or 0.5 spike/s, if no spikes occurred). Threshold was taken as the median of three independent runs.

Rate-intensity experiment

Pure tones of 100 ms at the CF were presented at eight different sound levels, and the spike rates were averaged over ten presentations. Levels were increased successively by 4 dB steps. Spontaneous activity was averaged over 125 ms preceding all 80 stimulus presentations. Natural call stimuli were presented similarly.

Response area experiment

Spikes were counted while 50 ms tone bursts were systematically varied in frequency and level, in pseudorandom order. The variation encompassed ten levels in 6 dB increments and 30 frequencies in 1/6 octave steps.

Data analysis

To determine threshold, a cumulative normal distribution was fit by a least-squares method to the spike-rate stimulus-response curve measured from at least ten pure-tone CF presentations at eight different intensities (Kanneworff 2004). Spontaneous firing rate figured as a constant, and fit parameters were the mean and standard deviation of intensity at the midpoint of increase in firing rate, and the saturation discharge rate. We defined threshold at 5% of the distance up the firing-rate ordinate from the spontaneous to the saturation rate. The normal distribution function gave a better fit (*F* test) to a randomly chosen sample of our cells than sigmoidal or standard logistic functions used previously (Yates et al. 1990; Tougaard 1996; Nizami 2002; Kanneworff 2004). Dynamic range was the range of stimulus intensity within one standard deviation of the intensity at the spike-rate curve midpoint. Median latencies of the first poststimulus spikes were fit by least-squares to an exponential decay model, $Y = L_{min} + (L_{max} - L_{min}) \times {}^{-b(X-\text{threshold})}$, with latency Y, stimulus intensity X, minimum latency L_{min}, and latency at threshold L_{max} (Imaizumi and Pollack 2001; Kanneworff 2004).

Phasic-tonic response characteristics to pure tones were quantified by the index $(S_1 - S_2)/(S_1 + S_2)$ where S_1 is the number of spikes in the first 40 ms after tone onset, and S_2 is the number of steady-state spikes in the last 40 ms of the tone (Megela and Capranica 1981, 1982; Hall and Feng 1988). Using this index, 1 represents a phasic response during only the initial 40 ms, 0 represents an ideally tonic response, and −1 represents a response in only the later 40 ms.

Our correlation analysis measured the similarity in temporal pattern between responses and the call stimuli. The call signal envelope $E(t)$ was extracted using the Hilbert transform. Each stimulus envelope was cross-correlated with the poststimulus time histogram (PSTH, 0.5 ms bin width) of the spike trains (Louage et al. 2004). We smoothed the cross-correlation function (CCF) and normalized it by the maximal attainable cross-correlation value, CCF_{max}. The scaling factor CCF_{max} is obtained by calculating the $CCF_{ideal}(t)$ for a model cell with the same spike rate as the actual cell but with ideally timed spikes making its PSTH a scaled version of the signal envelope:

$$\text{PSTH}(t) = A \times E(t).$$

The $CCF_{ideal}(t)$ is proportional to the autocorrelation of the envelope (ACF):

$$CCF_{ideal}(t) = A \times ACF(t)$$

where

$$A = \int_0^T \text{PSTH}(t) / \int_0^T E(t)\, \mathrm{d}t$$

for stimulus duration T, and

$$\text{CCF}_{max} = A \times \text{ACF}_{max} = \text{ACF}_{max} \times \int_0^T \text{PSTH}(t)/\int_0^T E(t)\,\mathrm{d}t.$$

Thus, the normalized CCF measures temporal coding independent of spike rate and stimulus power.

The normalized cross-correlation yielded a quasi-periodic function scaled from −1 to 1 with peaks at negative as well as positive delays, due to the periodicity of the call envelopes. To correct for high-normalized CCF values at low spike rates, we subtracted as a baseline the "background CCF" of a PSTH with the same number of spikes randomly shuffled. The delay of CCF_{max} corresponds to spike latency in our interpretation. We extracted for analysis the normalized CCF_{max} lying within a positive delay of 100 ms. Data analysis used custom-made software ('RetrieveMaster') and a vector processing programming toolbox (OptiVec, Martin Sander Inc.).

Results

Characteristic firing patterns of primary afferents and DMN neurons

Spontaneous activity was determined for 297 auditory nerve (n.VIII) fibers (Fig. 2a). Spontaneous firing rates, recorded for 2 s before each frequency-tuning test, ranged from 0.2 to 80 spikes/s. Most fibers had relatively low spontaneous rates (median: 2.4 spikes/s; 50% of the values fell between 0.9 and 9 spikes/s). The range of spontaneous rates is broad across fibers of all threshold sensitivities. Nonetheless, there is a weak (−0.459 dB/(spikes/s) but significant ($P < 0.001$) correlation between the spontaneous rates of nerve fibers and their thresholds at CF (not shown), indicating that cells with high spontaneous activity have somewhat lower thresholds (coefficient of determination r^2 of 0.211 with a regression slope of −0.753 dB/(spikes/s)).

We also recorded from 253 DMN units at electrode depths between 10 and ~500 μm. The range of spontaneous rates in the DMN was 0.2 to 73 spikes/s with a median value of 0.8 spikes/s; 50% of all values were between 0.5 and 3.5 spikes/s (Fig. 2a). Thus, the spontaneous firing rates of DMN neurons closely resemble those of their afferents. The negative correlation between spontaneous rate and threshold was weaker in the DMN (−0.084, $P < 0.005$, r^2 of 0.032).

A CF was determined for each unit and a frequency tuning curve (FTC) constructed (Fig. 3). For n.VIII (Fig. 3a), typical FTCs are broad. Curves may be double peaked, peaked with shoulders, symmetrical or asymmetrical (Fig. 3a). In the DMN (Fig. 3b), FTCs are similarly broad and include the same types as were found in the nerve. Values of Q_{10} (the bandwidth of the FTC 10 dB above threshold) averaged 1.9 ± 1.4 (mean ± SD) in the nerve (range 0.5–8.3), and 1.5 ± 1.1 in the DMN (range 0.3–9.5). There was no systematic relation between CF and Q_{10} (coefficient of determination $r^2 = 0.009$).

The distribution of CFs in the nerve and the DMN is illustrated in Fig. 4. The range of CFs is the same in both locations. In the nerve, there are two peaks in the distribution of CFs at around 200 and 600 Hz, and a third peak at around 1,500 Hz. In the DMN, CFs are broadly distributed with two peaks around 200 and 500 Hz, but lesser representation in the higher frequency range. The distribution of CFs may be related to frequency representations in the amphibian and basilar papillae (AP and BP, respectively). Based on the 496:310 proportion of fibers counted by Dunn and Will (Will and Fritzsch 1988), 38% of fibers originate in the

BP; in our population of nerve recordings, 38% lie above 700 Hz (approximated by dashed reference line, Fig. 4). In contrast, DMN CFs above 700 Hz comprise only 19% of the DMN unit recordings. The paucity of high-frequency units in the DMN relative to the nerve indicates either a sampling bias against units with higher CFs, or a genuine difference in frequency representation throughout the DMN. No dorsoventral tonotopy was noted with recording depth for either the nerve or the DMN.

The broad range of CFs we measured across the population of *X. laevis* n.VIII fibers could have obscured a narrower tuning of presumed BP fibers within individuals. To compare inter- and intra-animal variability, we examined the interquartile range of CFs above 1 kHz in eight frogs (Fig. 2b). The 8 individuals were selected because we recorded at least five units with CFs above 1 kHz in each. From the F ratio (one-way ANOVA) for the >1 kHz CF distribution, 1.46, we estimate that the variability between individuals is about half the variance within individuals (the F ratio is the ratio of between-individual variance to within-individual variance; and between-individual variance is the sum of inherent variation and variation attributable to differences among individual sample means, King and Minium 2003). The null hypothesis that all individuals had the same mean CF could not be rejected, $P = 0.19$. Thus, tuning of presumed BP fibers within individuals does not appear narrower than tuning across individuals.

Thresholds of units in n.VIII (Fig. 5) ranged from −100 to 4 dB re an eardrum vibration velocity of 1 mm/s. We compared thresholds in two females and two males with comparable numbers of fibers recorded (68 in total, females; 67, males). Across the whole population of recordings, the mean thresholds were not significantly different between the sexes (not shown; 64–205 Hz thresholds, $P = 0.57$; 206–705 Hz, thresholds, $P = 0.87$; 706–3260 Hz thresholds, $P = 0.30$). In the DMN (Fig. 6), thresholds ranged from −99 to 7 dB re 1 mm/s. We tested for gender differences in DMN frequency sensitivity and found none significant ($P = 0.14$ for thresholds of cells with CFs under 205 Hz; $P = 0.72$ for cells between 206 and 705 Hz; $P = 0.44$ for cells above 705 Hz).

Spike rate-intensity curves at CF are monotonic, whether sloping or saturating (not illustrated). The mean dynamic range was 21.1 ± 9.3 dB re 1 mm/s in the n.VIII, and 23.7 ± 12.2 dB in the DMN, with greatest dynamic ranges of 59.7 dB in the n.VIII and 75.8 dB in the DMN. Unlike in the mammalian auditory nerve (Taberner and Liberman 2005), dynamic range did not decrease with spontaneous rate. When different frequency tones are presented at sound levels much louder than the minimum threshold, higher or lower frequencies can sometimes evoke more spikes than the CF (Fig. 7a-middle panel, b-upper panel). Most nerve and DMN units respond monotonically with intensity at frequencies other than CF (Fig. 7a-middle and lower panel, b-middle panel). Occasional units (Fig. 7a-upper panel) give a maximal response near threshold, so that as the sound level increases, the firing rate decreases.

In response to pure tones (Fig. 2c), some neurons fire throughout the stimulus (a tonic response pattern) whereas others fire only once at tone onset (phasic) or give short bursts of spikes at the beginning of the tone (phasic burst). Phasic-tonic index values are somewhat more phasic in the DMN than in the nerve (Fig. 2c) and some offset cells were noted (Fig. 2c). When the response latencies to pure tones of varying intensities at CF were fit with an exponential decay, the mean minimum latency in the auditory nerve was 7.2 ms, whereas in the DMN the minimum latency averaged 9.0 ms.

DMN temporal discharge patterns can be grouped into categories similar to those described by Hall and Feng (1990). To examine whether responses showed classical chopping

patterns, we measured a synchronization index by taking the spectrum of the autocorrelation of smoothed PSTHs in response to ten presentations of CF tones 10–13 dB above threshold, and then normalizing by the mean spike rate. Out of 192 cells, 129 primary-like cells showed peak frequencies near that of the stimulating CF pure tone; 43 choppers had synchronization indices representing frequencies far from an integer multiple of the stimulus period. In addition to these two categories, we saw purely phasic, phasic burst, and offset response patterns: there were 5 purely phasic neurons; 14 phasic-burst cells synchronized to varying degrees but adapted after firing a few spikes; and there was one offset cell. Most choppers continued to fire throughout the 100-ms tone.

Call responses of auditory nerve fibers and DMN neurons

When call stimuli are presented, the timing of spikes is matched to the temporal pattern of the call envelope, regardless of the particular CF or whether the cell's temporal response pattern to tones is more phasic or tonic (Fig. 8). The temporal representation of the click envelope was sharpened by postexcitatory suppression in some n.VIII units (postexcitatory suppression is apparent following the pure tone burst of cell 1 in Fig. 8; when CF tones were presented at 13 increasing levels from threshold to 50 dB above, the mean spontaneous rate of this unit decreased from 13.2 spikes/s in the 135 ms preceding the tone to 1.1 spikes/s in the 135 ms after the tone).

We used a cross-correlation (CC) analysis to quantify the temporal similarity of the PSTHs to the call envelopes (Fig. 9) (Louage et al. 2004). Normalized CC functions show a clear maximum peak with characteristic latency for responses to all stimuli (Fig. 9). Lesser peaks at other time delays occur because the stimulus is periodic. When 114 nerve fibers were presented with the slow advertisement call stimulus 10–30 dB above threshold at CF, the average CC peak was 0.54 ± 0.21 s.d., indicating a precise temporal representation (average peak latency 4.8 ± 7.7 ms). In 48 DMN cells, the corresponding average CC peak was 0.45 ± 0.24 s.d. The normalized CC peaks were lower in response to the fast trill of the advertisement call (Fig. 9); due to the high sound energy during most of the stimulus, the background CCFs of randomized spikes used for normalization were high (see "Materials and methods"). For stimuli containing longer interclick intervals, such as rapping and ticking, background CCFs were lower, producing higher normalized CC peaks (not shown). At high sound levels, temporal representations may degrade. For example, when double-spiking occurs in response to single clicks, the representation of click time is ambiguous. Firing in all units, whether in the nerve or in the DMN, correlates highly with click timing in each call. The ability of 114 nerve units to follow slow advertisement click trains is not related to CF (coefficient of determination $r^2 = 0.01$), phasic-tonic index ($r^2 = 0.03$), or threshold ($r^2 = 0.005$). Nerve fibers with higher spontaneous activity had somewhat lower CC peaks to the slow advertisement trill ($r^2 = 0.23$, slope of -0.007, $P < 0.0001$) than other fibers. In 48 DMN units, units with higher phasic-tonic indices had somewhat higher CC peaks to the slow advertisement trill ($r^2 = 0.22$, slope of 0.30, $P < 0.001$). But their CC peaks had no relation to the CF ($r^2 = 0.008$), threshold ($r^2 = 0.003$), or SR ($r^2 = 0.01$).

Discussion

This study is the first detailed account of peripheral and hindbrain auditory responses in the fully aquatic anuran *X. laevis*, a species in which vocal behavior plays a prominent role in social communication (Tobias et al. 1998, 2004). We devised a method of directly stimulating the tympanum that allows us to present clean tympanic stimuli that match underwater sounds in frequency and sound level, and can be quantitatively compared to laser vibrometry measurements of the tympanum during underwater sound broadcasts (Christensen-Dalsgaard and Elepfandt 1995). We tested both classical frequency tuning and

firing pattern characteristics, in addition to the processing of click patterns in conspecific calls. Our results show that single units in the auditory nerve and DMN are highly sensitive to tympanic stimulation, showing V-shaped tuning curves and best sensitivities of −101 dB re 1 mm/s. In both sexes, neural representations at these early stages of auditory processing faithfully preserve the temporal features of natural calls.

Auditory specializations: the ear and the papillae

A suite of anatomical features of the ear in *Xenopus* suggest adaptations for waterborne hearing. For example, the movement of the stiff cartilaginous tympanum as a plate in *Xenopus* may be better suited to underwater sound detection than the buckling vibrational modes of flexible tympanic membranes in birds and mammals (Christensen-Dalsgaard and Elepfandt 1995). Also, vibration of the *X. laevis* tympanum is constrained within the membranous frame of the annulus, and the connection between the air cavities that drive the two tympana from within may allow for directional hearing underwater (Christensen-Dalsgaard and Elepfandt 1995).

The distribution of frequency tuning in the higher-frequency auditory epithelium of *X. laevis*, the BP (Wever 1985), may be adapted for detecting the peak energy in *Xenopus* calls (1.2–1.6 kHz). These dominant frequencies in *X. laevis* calls are higher than dominant peaks in calls of comparably sized terrestrial frogs (Zakon and Wilczynski 1988). Will and Fritzsch (1988) showed that the auditory epithelia in *X. laevis* have a higher proportion of BP fibers to AP fibers (3:5) than exists in for example *R. catesbeiana* (1:4) and *B. orientalis* (1:4), perhaps reflecting a bias towards higher frequencies. In our population of recorded fibers, 38% of the CFs, which corresponds to the published BP fiber ratio (Will and Fritzsch 1988), lie between 705 and 3,250 Hz, and we presume that most of the group above 1 kHz originates in the BP. This range may be an underestimate since we probably missed fibers with tuning curves entirely above 3,200 Hz, the upper limit of our search sweep.

The BP fiber recordings in terrestrial frogs have found a small range of best frequencies within individuals, a relatively small number of hair cells, a linear response to stimulus intensity, and no increase of best frequency with temperature (Capranica and Moffat 1977; Megela and Capranica 1982; Ehret et al. 1983; van Dijk et al. 1990). Such results led to the suggestion that the BP functions as a simple mechanical resonator (Zakon and Wilczynski 1988). However, in *Xenopus* we measured a broad range of >1 kHz CFs within individuals, which does not support a simple oscillator model of the BP.

Some evidence under different protocols indicates *Xenopus* have finer behavioral discrimination of higher frequencies than terrestrial frogs (Fay and Simmons 1999; Elepfandt et al. 2000), an ability that could be related to a diversity of BP tuning (Fig. 2b) and a relatively high proportion of BP fibers (Will and Fritzsch 1988) (Fig. 4). The disparity in high frequency discrimination may represent different selective pressures in terrestrial and aquatic habitats. In shallow water, depth limits how far low fundamental frequencies propagate, with a cut-off frequency of 1 kHz in a pond typical of *Xenopus* habitat (clayey silt bottom, 2 m depth) (Rogers and Cox 1988), possibly forcing *Xenopus* sound communication and hearing into higher frequencies.

Although *X. laevis* clicks differ somewhat in frequency by sex (1.2 kHz in females vs. 1.6–1.8 kHz in males), we found no significant gender difference in n.VIII frequency sensitivities. In contrast, the peripheral auditory sensitivity of the tree frog *Eleutherodactylus coqui* is sexually dimorphic (Narins and Capranica 1976).

Underwater audiogram estimation and comparison to earlier measurements

Since the transfer function between underwater sound and tympanic vibration has been measured previously (Christensen-Dalsgaard and Elepfandt 1995), the sensitivity to tympanic vibration we measured can be recalculated as equivalent natural aquatic sound sensitivities, and an audiogram can be estimated in terms of underwater sound pressure (Fig. 10) from our CF-threshold data. We used Christensen-Dalsgaard and Elepfandt's laser measurements of tympanic vibration velocity (1995) in a female weighing 60.5 g. The average weight of the frogs from which we present nerve recordings was 64 g. By the transfer function, a 1.6 kHz tone at 10 Pa vibrates the tympanum at 3.2 mm/s. Therefore, sensitivity we measured at 1.6 kHz is equivalent to −77 dB re 1 Pa. The minimum threshold at 1.6 kHz was about 45 nm/s tympanic vibration velocity, corresponding to an underwater sound pressure level of 0.14 mPa. Two other regions of peak sensitivity in Fig. 10 are −90 dB re 1 Pa at 675 Hz, and −44 dB re 1 Pa at 2,975 Hz. The threshold peaks occur at roughly the same frequencies (after transformation to pressure dB) as peak auditory thresholds in behavioral conditioning (0.6, 1.6, and 3.4 kHz), frequency discrimination limens (0.6, 2 kHz) (Elepfandt et al. 2000), and cochlear microphonics (300–700 Hz and 1200–2500 Hz) (Wever 1985).

For the sake of comparison with other small aquatic vertebrates, the most sensitive behavioral audiograms from ostariophysine fish (in which sound sensitivity is similarly 'amplified' by coupling of the ear to an air-filled cavity) show maximum hearing thresholds at 1 kHz of −65 dB re 1 Pa (Fay and Simmons 1999). When a relatively sensitive goldfish audiogram (Popper 1971; Fay 1988) is compared to the audiogram of terrestrial frogs (e.g. Christensen-Dalsgaard et al. 1998) the thresholds are similar in terms of sound pressure (Fig. 10). This observation may initially be surprising, since *Xenopus* is then much more sensitive in terms of sound intensity, which is the relevant parameter for direct comparisons between underwater and air thresholds (Møhl 1968). However, the similarity in sound pressure sensitivities is probably due to the *Xenopus* ear being driven by aerial sound pressure in its cavity, like the ranid ear (Lombard et al. 1981). Previous estimates of the *Xenopus* hearing range in air (0.2–3.5 kHz) and peak sensitivity (between 1.2 and 2 kHz; Hetherington and Lombard 1982; van Dijk et al. 2002; Bibikov and Elepfandt 2005; Katbamna et al. 2006) are fairly compatible with the total range and peak sensitivity of our CF measurements.

Neural sensitivity to natural calls

The frequency sensitivities of the eighth nerve match the broadband spectral energy in conspecific male and female vocalization clicks, with a peak in the CF distribution between 1.2 and 1.8 kHz. Cells with CFs lower than 1.2 kHz are tuned broadly enough to respond to a call stimulus at relatively low sound levels. Depending on CF, the click intensity that reliably elicits spiking lies around 10–40 dB above the pure CF tone level that consistently elicits spikes. The amplitude of the advertisement call 2 cm in front of the snout of adult *X. laevis* males is 45 dB re 1 Pa (Elepfandt 1996). Across the greatest extent of one fairly typical 44 m long and over 2 m deep breeding pond near Cape Town, South Africa (Tobias et al. 2004), such a call would fall to 12 dB re 1 Pa, assuming cylindrical spreading (3 dB per distance doubling). At that level, the dominant frequency of the male click, 1.6 kHz, would produce a tympanic vibration of 3.9 mm/s, well above the least sensitive thresholds we measured. In the recording sessions from which our female stimuli were taken, the quietest female ticking call had an amplitude of −81 dB at 1 Pa at an unknown distance in the 44 m pond (Tobias et al. 1998). In the shallow habitat of *X. laevis*, signals are high-pass filtered so that in areas of 2 m depth, frequencies under 1 kHz do not propagate far and are probably best suited for short-range communication (Picker 1983; Rogers and Cox 1988; Tobias et al. 2004).

Basic nerve response characteristics in *X. laevis* and other anurans

Responses of eighth nerve fibers have been characterized in a variety of anuran species. Christensen-Dalsgaard et al. (1998) found spontaneous rates in the ranid eighth nerve up to 75 spikes/s, as did we in *X. laevis*, but in other terrestrial frogs the spontaneous rates reported have been much lower, probably reflecting differences in anesthetic and surgical procedures (Christensen-Dalsgaard et al. 1998).

The range of frequency sensitivities in the periphery of *X. laevis* extends somewhat lower than the minimum CF in *H. cinerea* (100 Hz) (Moffat and Capranica 1974), and higher than the maximum in *Rana* (1800 Hz) (Frishkopf and Geisler 1966; Feng et al. 1975; Megela and Capranica 1981). The vast majority of rate-intensity slopes in the eighth nerve have monotonic shapes, as in ranids; slopes of rate-intensity curves from nerve fibers in *R. pipiens* typically range, as ours did, from 2 to 12 spikes/(s dB) (Feng 1982). As in *R. temporaria* (Christensen-Dalsgaard et al. 1998), some *Xenopus* afferent fibers show postexcitatory suppression of their spontaneous activity. The maximum Q_{10} value that we measured in the nerve, 8.3, equals the maxima from terrestrial frogs, with the difference that we found tuning to be equally sharp in the BP range (Megela and Capranica 1981; Zakon and Wilczynski 1988).

In *Xenopus*, eighth nerve temporal discharge patterns to tonal stimulation were diverse in fibers in every region of frequency tuning. In *H. cinerea* and *R. pipiens*, in contrast, only tonic PSTH profiles are found in BP fibers, and more peaked PSTHs at higher CFs within the AP range (Megela and Capranica 1981).

Comparison of basic response characteristics in the DMN

The DMN spontaneous rates up to 43 spikes/s have been reported in *R. pipiens* (Hall and Feng 1990), whereas we found rates up to 73 spikes/s. DMN rate-intensity curves have slightly shallower slopes in *Xenopus* than in Ranids (Christensen-Dalsgaard et al. 1998); our measurements typically ranged from 1 to 10 spikes/(s dB). The median dynamic range we measured in the DMN was 20 dB. In the DMN of *Rana*, previously reported Q_{10}s are similarly broad (1.8 mean ± 1.2 S.D.) but the upper limit of their range (maximum 4) (Hall and Feng 1990) stops short of our sharpest DMN Q_{10} values in the AP range (maximum 9.5).

The *Xenopus* DMN population of CFs has a higher frequency range than the ranid population (van Stokkum 1987; Hall and Feng 1990). DMN Q_{10}s correlate positively with CF and negatively with threshold in ranids (Hall and Feng 1990) whereas we found no correlation in *X. laevis*. We found no tonotopy along the dorsoventral axis of the DMN, a feature described in *R. pipiens* (Fuzessery and Feng 1981). DMN spontaneous firing rates are low in both species, but we did not find higher thresholds in neurons with low spontaneous firing rates as described in *R. pipiens* (Hall and Feng 1990). Finally, if some of the cells in the *Xenopus* DMN require binaural input (Feng and Capranica 1976; Feng and Schellart 1999), we may have failed to stimulate these cells satisfactorily. Most likely, such binaural cells will have 'normal' excitatory tuning curves when stimulated monaurally (Christensen-Dalsgaard and Kanneworff 2005).

The percentages of units having different categories of temporal discharge patterns in the DMN of *Xenopus* differ only somewhat from the percentages in *R. pipiens* (Hall and Feng 1990). We found slightly fewer phasic and phasic burst units (10% in total) than were reported in *Rana* (16%); and roughly the same prevalence of choppers (22%) as that identified in *Rana* when some responses at levels >10 dB above threshold are included (25%).

Encoding of natural vocalizations

The firing pattern of eighth nerve fibers in the periphery represents the envelope of calls, without any selectivity for call type beyond the subtle threshold biases related to frequency tuning. However, postexcitatory suppression reduces the firing during the lower amplitudes of the call envelope, sharpening the temporal representation of the envelope in the *Xenopus* auditory nerve, as in *R. temporaria* (Christensen-Dalsgaard et al. 1998).

Temporal coding has classically been examined using synthetic stimuli, which gives envelope-detecting and fine structure cutoffs that can be compared with conspecific calls. Auditory nerve fibers in terrestrial frogs phase-lock to sine amplitude-modulated tones, relatively unaffected by manipulation of modulation depth and sound level (Rose and Capranica 1985; Schwartz and Simmons 1990; Klump et al. 2004), just as auditory nerve fibers time-lock indiscriminately to call pulses (Feng et al. 1991; Klump et al. 2004). This response feature is shared by the aquatic *X. laevis*.

In *X. laevis*, DMN responses to rapid click rates, like responses in the eighth nerve, are also phase-locked. All cells can follow overlapping 63-Hz clicks in the fast trill of the male advertisement call, as predicted by reports of brainstem auditory evoked potentials (Bibikov and Elepfandt 2005). In contrast, some DMN neurons in terrestrial frogs exhibit band-pass characteristics, selecting with mean spike count for AM rates between 10 and 40 Hz (Hall and Feng 1991; Feng and Lin 1994).

In both the *X. laevis* eighth nerve and the DMN, either a single spike or a burst of spikes encodes each click. Response patterns across the population correlate highly with the temporal envelope of natural call stimuli, whether cells show high or low spontaneous activity, or phasic or sustained responses to tones. Since there is no filtering for click rate at the level of the auditory nerve or DMN, selectivity for specific calls must occur higher in the central auditory system (as we have examined in the TS) (Elliott 2007).

Acknowledgments

Abbreviations

ACF	Autocorrelation function
AM	Amplitude modulation
AP	Amphibian papilla
BP	Basilar papilla
CC	Cross-correlation maximum
CCF	Cross-correlation function
CF	Characteristic frequency

dB	Decibels
DMN	Dorsal medullary nucleus
DPOAE	Distortion product otoacoustic emissions
FTC	Frequency–threshold curve
n.VIII	Auditory nerve
PSTH	Poststimulus time histogram
Q_{10}	Tuning quality factor
SR	Spontaneous rate
TS	Torus semicircularis

References

Bentley PJ, Shield JW. Respiration of some urodele and anuran amphibia part 2: in air role of the skin and lungs. Comp Biochem Physiol A. 1973; 46:29–38. [PubMed: 4147801]

Bibikov NG, Elepfandt A. Auditory evoked potentials from medulla and midbrain in the clawed frog, *Xenopus laevis laevis.* Hear Res. 2005; 204:29–36. [PubMed: 15925189]

Bodnar DA, Capranica RR. Encoding of phase spectra by the peripheral auditory system of the bullfrog. J Comp Physiol A. 1994; 174:157–171. [PubMed: 8145188]

Capranica, RR. Morphology and physiology of the auditory system. In: Llinás, R.; Precht, W., editors. Frog neurobiology: a handbook. Springer; New York: 1976. p. 551-575.

Capranica RR, Moffat AJ. Place mechanism underlying frequency analysis in the toad's inner ear. J Acoust Soc Am. 1977; 62:S36.

Christensen-Dalsgaard J, Narins PM. Sound and vibration sensitivity of VIIIth nerve fibers in the frogs *Leptodactylus albilabris* and *Rana pipiens pipiens.* J Comp Physiol A. 1993; 172:653–662. [PubMed: 8350283]

Christensen-Dalsgaard J, Elepfandt A. Biophysics of underwater hearing in the clawed frog, *Xenopus laevis.* J Comp Physiol A. 1995; 176:317–324. [PubMed: 7707269]

Christensen-Dalsgaard J, Jørgensen MB, Kanneworff M. Basic response characteristics of auditory nerve fibers in the grassfrog (*Rana temporaria*). Hear Res. 1998; 119:155–163. [PubMed: 9641328]

Christensen-Dalsgaard J, Kanneworff M. Binaural interaction in the frog dorsal medullary nucleus. Brain Res Bull. 2005; 66:522–525. [PubMed: 16144642]

Edwards CJ, Kelley DB. Auditory and lateral line inputs to the midbrain of an aquatic anuran: neuroanatomic studies in *Xenopus laevis.* J Comp Neurol. 2001; 438:148–162. [PubMed: 11536185]

Ehret G, Moffat AJ, Capranica RR. Two-tone suppression in auditory nerve fibers of the green treefrog (*Hyla cinerea*). J Acoust Soc Am. 1983; 73:2093–2095. [PubMed: 6875094]

Elepfandt, A. Underwater acoustics and hearing in the clawed frog, *Xenopus*. In: Kobel, HR.; Tinsley, R., editors. The biology of Xenopus. Vol. 68. Symp. Zool. Soc. London; London: 1996. p. 177-193.

Elepfandt A, Eistetter I, Fleig A, Gunther E, Hainich M, Hepperle S, Traub B. Hearing threshold and frequency discrimination in the purely aquatic frog *Xenopus laevis* (Pipidae): measurement by means of conditioning. J Exp Biol. 2000; 203(Pt 23):3621–3629. [PubMed: 11060223]

Elliott, TM. Doctor of Philosophy, Graduate School of Arts and Sciences. Columbia University; New York: 2007. The neural basis of click rate coding in the auditory system; p. 145

Elliott TM, Kelley DB. Male discrimination of receptive and unreceptive female calls by temporal features. J Exp Biol. 2007; 210:2836–2842. [PubMed: 17690231]

Evans BJ, Kelley DB, Tinsley RC, Melnick DJ, Cannatella DC. A mitochondrial DNA phylogeny of African clawed frogs: phylogeography and implications for polyploid evolution. Mol Phylogenet Evol. 2004; 33:197–213. [PubMed: 15324848]

Fay, RR. Hearing in vertebrates: a psychophysics databook. Hill-Fay; Winnetka: 1988.

Fay, RR.; Simmons, AM. The sense of hearing in fishes and amphibians. In: Fay, RR.; Popper, AN., editors. Comparative hearing: fish and amphibians. Vol. 11. Springer; New York: 1999. p. 269-318.

Feng AS, Narins PM, Capranica RR. Three populations of primary auditory fibers in the bullfrog (*Rana catesbeiana*): their peripheral origins and frequency sensitivities. J Comp Physiol A Neuroethol Sens Neural Behav Physiol. 1975; 100:221–229.

Feng AS, Capranica RR. Sound localization in anurans. I. Evidence of binaural interaction in dorsal medullary nucleus of bullfrogs (*Rana catesbeiana*). J Neurophysiol. 1976; 39:871–881. [PubMed: 1085815]

Feng AS. Quantitative analysis of intensity-rate and intensity-latency functions in peripheral auditory nerve fibers of northern leopard frogs (*Rana p. pipiens*). Hear Res. 1982; 6:241–246. [PubMed: 6979535]

Feng AS, Hall JC, Siddique S. Coding of temporal parameters of complex sounds by frog auditory nerve fibers. J Neurophysiol. 1991; 65:424–445. [PubMed: 2051189]

Feng AS, Lin WY. Phase-locked response characteristics of single neurons in the frog "cochlear nucleus" to steady-state and sinusoidal-amplitude-modulated tones. J Neurophysiol. 1994; 72:2209–2221. [PubMed: 7884454]

Feng, AS.; Schellart, NAM. Central auditory processing in fish and amphibians. In: Fay, RR.; Popper, AN., editors. Comparative hearing: fish and amphibians. Vol. 11. Springer; New York: 1999. p. 218-268.

Frishkopf LS, Geisler CD. Peripheral origin of auditory responses recorded from the eighth nerve of the bullfrog. J Acoust Soc Am. 1966; 40:469–472.

Fuzessery ZM, Feng AS. Frequency representation in the dorsal medullary nucleus of the leopard frog, *Rana p. pipiens*. J Comp Physiol A Neuroethol Sens Neural Behav Physiol. 1981; 143:339–347.

Gerhardt, HC.; Schwartz, JJ. Auditory tuning and frequency preferences in anurans. In: Ryan, MJ., editor. Anuran communication. Smithsonian Institution Press; Washington: 2001. p. 73-85.

Gerhardt, HC.; Huber, F. Acoustic communication in insects and anurans. University of Chicago Press; Chicago: 2002.

Hall JC, Feng AS. Influence of envelope rise time on neural responses in the auditory system of anurans. Hear Res. 1988; 36:261–276. [PubMed: 3209496]

Hall JC, Feng AS. Classification of the temporal discharge patterns of single auditory neurons in the dorsal medullary nucleus of the northern leopard frog. J Neurophysiol. 1990; 64:1460–1473. [PubMed: 2283537]

Hall JC, Feng AS. Temporal processing in the dorsal medullary nucleus of the Northern leopard frog (*Rana pipiens pipiens*). J Neurophysiol. 1991; 66:955–973. [PubMed: 1661327]

Hetherington TE, Lombard RE. Biophysics of underwater hearing in anuran amphibians. J Exp Biol. 1982; 98:49–66. [PubMed: 6980964]

Imaizumi K, Pollack GS. Neural representation of sound amplitude by functionally different auditory receptors in crickets. J Acoust Soc Am. 2001; 109:1247–1260. [PubMed: 11303938]

Jørgensen MB, Christensen-Dalsgaard J. Directionality of auditory nerve fiber responses to pure tone stimuli in the grassfrog, *Rana temporaria*. I. Spike rate responses. J Comp Physiol A. 1997; 180:493–502. [PubMed: 9163927]

Kanneworff, M. Neural processing of directional cues in the frog dorsal medullary nucleus. PhD, Center for Sound Communication, Institute of Biology, Faculty of Science and Engineering, University of Southern Denmark; Odense, Denmark: 2004. p. 100

Katbamna B, Brown JA, Collard M, Ide CF. Auditory brainstem responses to airborne sounds in the aquatic frog *Xenopus laevis*: correlation with middle ear characteristics. J Comp Physiol A Neuroethol Sens Neural Behav Physiol. 2006; 192:381–387. [PubMed: 16322997]

Kelley, DB.; Tobias, ML. Vocal communication in *Xenopus laevis*. In: Hauser, MD.; Konishi, M., editors. The design of animal communication. MIT; Cambridge: 1999. p. 9-35.

King, BM.; Minium, EW. Statistical reasoning in psychology and education. Wiley; Hoboken: 2003.

Klump GM, Benedix JH Jr, Gerhardt HC, Narins PM. AM representation in green treefrog auditory nerve fibers: neuroethological implications for pattern recognition and sound localization. J Comp Physiol A Neuroethol Sens Neural Behav Physiol. 2004; 190:1011–1021. [PubMed: 15480704]

Levitt H. Transformed up–down methods in psychoacoustics. J Acoust Soc Am. 1971; 49(Suppl 2): 467. [PubMed: 5541744]

Lombard RE, Fay RR, Werner YL. Underwater hearing in the frog, *Rana catesbeiana*. J Exp Biol. 1981; 91:57–71.

Louage DH, van der Heijden M, Joris PX. Temporal properties of responses to broadband noise in the auditory nerve. J Neurophysiol. 2004; 91:2051–2065. [PubMed: 15069097]

Lowe DA. Organisation of lateral line and auditory areas in the midbrain of *Xenopus laevis*. J Comp Neurol. 1986; 245:498–513. [PubMed: 3517085]

Megela AL, Capranica RR. Response patterns to tone bursts in peripheral auditory system of anurans. J Neurophysiol. 1981; 46:465–478. [PubMed: 7299429]

Megela AL, Capranica RR. Differential patterns of physiological masking in the anuran auditory nerve. J Acoust Soc Am. 1982; 71:641–645. [PubMed: 7085968]

Moffat AJ, Capranica RR. Sensory processing in the peripheral auditory system of treefrogs (*Hyla*). J Acoust Soc Am. 1974; 55:480.

Møhl, B. Hearing in seals. In: Harrison, R.; Hubbard, R.; Rice, C.; Schusterman, RJ., editors. The behavior and physiology of pinnipeds. Appleton-Century; New York: 1968. p. 172-195.

Narins PM, Capranica RR. Sexual differences in the auditory system of the tree frog *Eleutherodactylus coqui*. Science. 1976; 192:378–380. [PubMed: 1257772]

Nizami L. Estimating auditory neuronal dynamic range using a fitted function. Hear Res. 2002; 167:13–27. [PubMed: 12117526]

Paton JA, Kelley DB, Sejnowski TJ, Yodlowski ML. Mapping the auditory central nervous system of *Xenopus laevis* with 2-deoxyglucose autoradiography. Brain Res. 1982; 249:15–22. [PubMed: 7139290]

Picker M. Hormonal induction of the aquatic phonotactic response of *Xenopus*. Behaviour. 1983; 84:74–90.

Popper AN. The effects of size on auditory capacities of the goldfish. J Audit Res. 1971; 11:239–247.

Rogers, PH.; Cox, M. Underwater sound as a biological stimulus. In: Atema, J.; Fay, RR.; Popper, AN.; Tavolga, WN., editors. Sensory biology of aquatic animals. Springer; New York: 1988. p. 131-149.

Rose GJ, Capranica RR. Sensitivity to amplitude modulated sounds in the anuran auditory nervous system. J Neurophysiol. 1985; 53:446–465. [PubMed: 3872351]

Schwartz JJ, Simmons AM. Encoding of a spectrally-complex communication sound in the bullfrog's auditory nerve. J Comp Physiol A. 1990; 166:489–499. [PubMed: 2332839]

Stevens CW, Klopp AJ, Facello JA. Analgesic potency of mu and kappa opioids after systemic administration in amphibians. J Pharmacol Exp Ther. 1994; 269:1086–1093. [PubMed: 8014851]

Taberner AM, Liberman MC. Response properties of single auditory nerve fibers in the mouse. J Neurophysiol. 2005; 93:557–569. [PubMed: 15456804]

Tobias ML, Viswanathan SS, Kelley DB. Rapping, a female receptive call, initiates male–female duets in the South African clawed frog. Proc Natl Acad Sci U S A. 1998; 95:1870–1875. [PubMed: 9465109]

Tobias ML, Barnard C, O'Hagan R, Horng SH, Rand M, Kelley DB. Vocal communication between male *Xenopus laevis*. Anim Behav. 2004; 67:353–365.

Tougaard J. Energy detection and temporal integration in the noctuid A1 auditory receptor. J Comp Physiol A. 1996; 178:669–677.

Trueb, L. Historical constraints and morphological novelties in the evolution of the skeletal system of pipid frogs (Anura: Pipidae). In: Tinsley, R.; Kobel, R., editors. The biology of Xenopus. Clarendon; Oxford: 1996. p. 349-377.

van Dijk P, Lewis ER, Wit HP. Temperature effects on auditory nerve fiber response in the American bullfrog. Hear Res. 1990; 44:231–240. [PubMed: 2329096]

van Dijk P, Mason M, Narins P. Distortion product otoacoustic emissions in frogs: correlation with middle and inner ear properties. Hear Res. 2002; 173:100. [PubMed: 12372639]

van Stokkum IH. Sensitivity of neurons in the dorsal medullary nucleus of the grassfrog to spectral and temporal characteristics of sound. Hear Res. 1987; 29:223–235. [PubMed: 3497912]

Vignal C, Kelley DB. Significance of temporal and spectral acoustic cues for sexual recognition in *Xenopus laevis*. Proc R Soc Lond B Biol Sci. 2007; 274:479–488.

Wever, EG. The amphibian ear. Princeton University Press; Princeton: 1985.

Will, U.; Fritzsch, B. The eighth nerve of amphibians. In: Fritzsch, B.; Ryan, MJ.; Wilczynski, W.; Hetherington, TE.; Walkowiak, W., editors. The evolution of the amphibian auditory system. Wiley; New York: 1988. p. 159-183.

Yager DD. Underwater acoustic communication in the African pipid frog *Xenopus borealis*. Bioacoustics. 1992; 4:1–24.

Yates GK, Winter IM, Robertson D. Basilar membrane nonlinearity determines auditory nerve rate-intensity functions and cochlear dynamic range. Hear Res. 1990; 45:203–219. [PubMed: 2358414]

Zakon, HH.; Wilczynski, W. The physiology of the anuran eighth nerve. In: Fritzsch, B.; Ryan, MJ.; Wilczynski, W.; Hetherington, TE.; Walkowiak, W., editors. The evolution of the amphibian auditory system. Wiley; New York: 1988. p. 125-155.
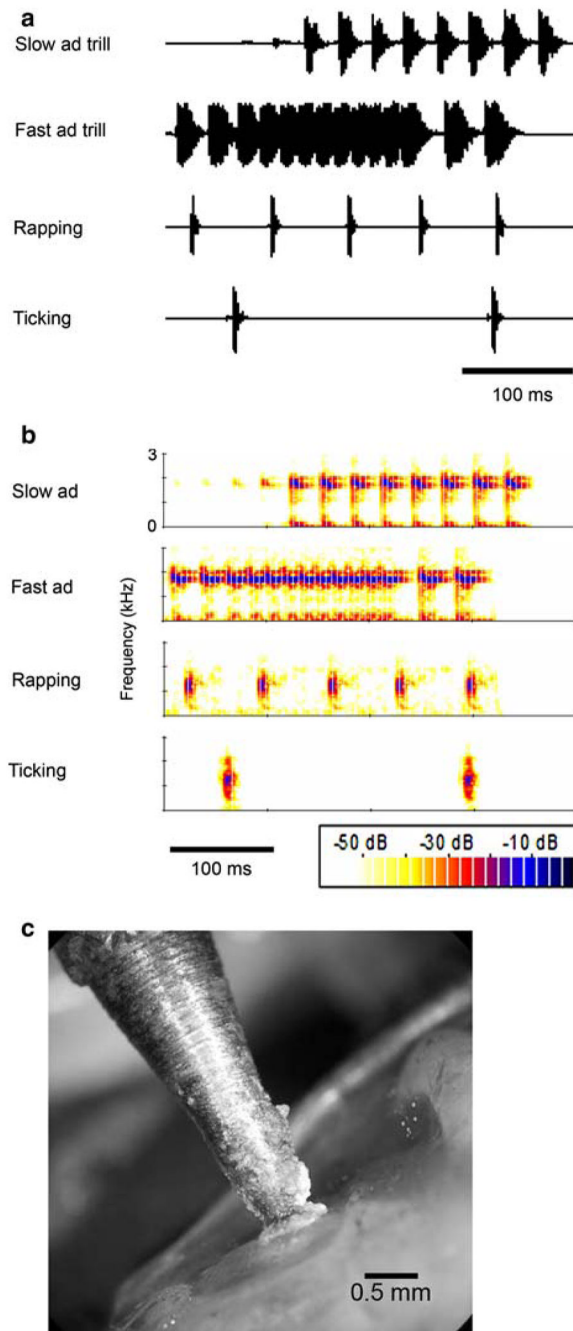
Fig. 1.
a Oscillograms of four 370 ms recorded call stimuli. The recording selections are representative of the natural calls' characteristic interclick intervals. Due to memory allocations in the custom-made stimulation program, the fast and slow trill portions of the male advertisement (ad) call were presented separately. For ticking, the 370 ms stimulus duration included just two clicks. **b** Spectrograms of the call stimuli in (**a**). The peak frequencies of clicks in the two female calls—rapping and ticking—are lower (1.2 kHz) than

the peak frequencies in the clicks of the male advertisement call (1.6–1.9 kHz). **c** The tip of the vibration-excited probe glued perpendicular to the center of the cartilaginous tympanum
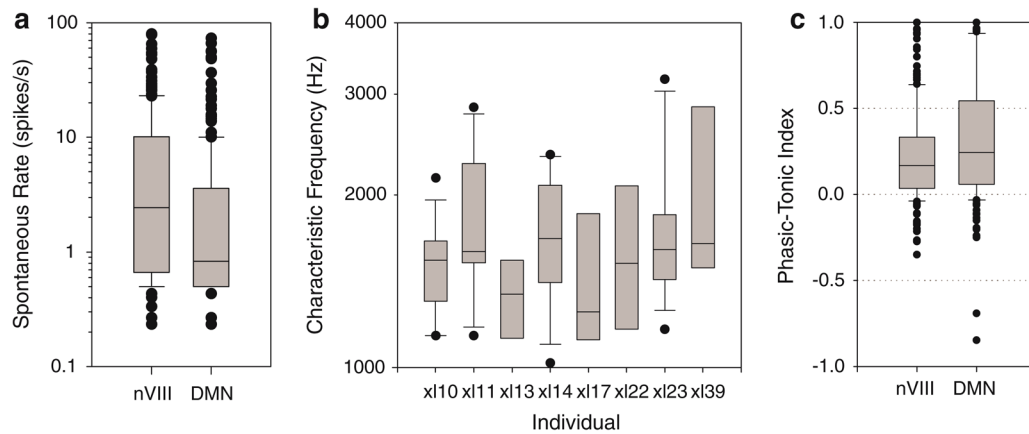
Fig. 2.
Boxplots in the figure show median and interquartile range (*boxes*), 10th and 90th percentiles (*whiskers*), and outliers (*dots*). **a** Distribution of spontaneous firing rates over 2 s intervals preceding 15 stimulations, depicted on a logarithmic axis, were somewhat higher in the nerve unit population than in the DMN. (Nerve: range from 0.2 to 79.5 spikes/s with a mean of 7.9 ± 12.5, $n = 283$. DMN: range from 0.2 to 73 with a mean of 4.4 ± 10 spikes/s, $n = 251$). **b** The within-individual distributions of nerve units with CFs above 1 kHz (eight individuals with at least five recordings; individuals with only five cells are represented only by median and interquartile range) are broader than the distributions previously reported in ranids (Zakon and Wilczynski 1988). **c** Phasic-tonic indices of temporal discharges in response to pure tones at CF in auditory nerve units and DMN units. The phasic-tonic index is $(S_1 - S_2)/(S_1 + S_2)$, where S_1 is the number of spikes in the first 40 ms after tone onset, and S_2 is the number of steady-state spikes in the last 40 ms of the tone stimulation. An index of 1 represents a phasic response occurring only in the initial 40 ms; 0 represents an ideally tonic response with equal numbers of spikes during the two 40 ms periods; and −1 represents a response in only the last 40 ms
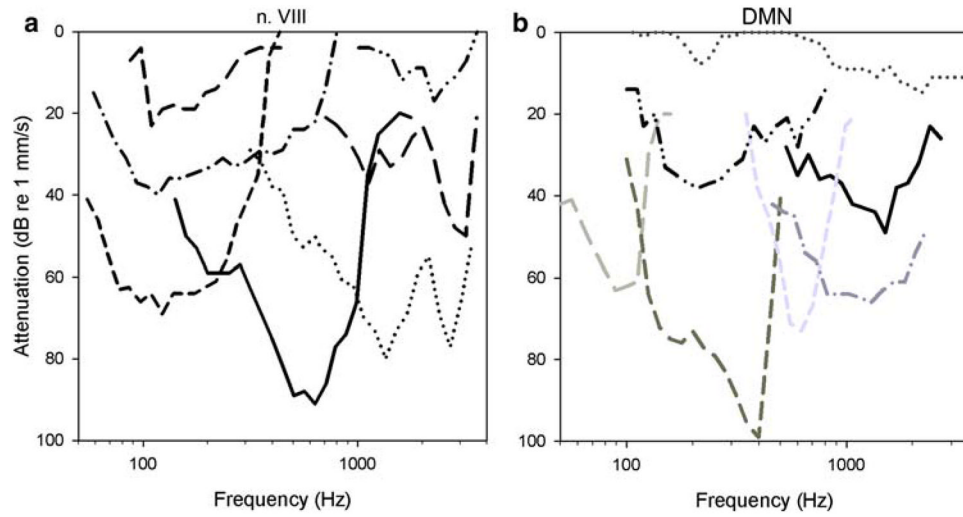
Fig. 3.
a Representative frequency tuning curves (FTCs) of seven auditory nerve units, selected to display the diversity of contours and bandwidths. **b** Similarly selected FTCs from seven DMN units
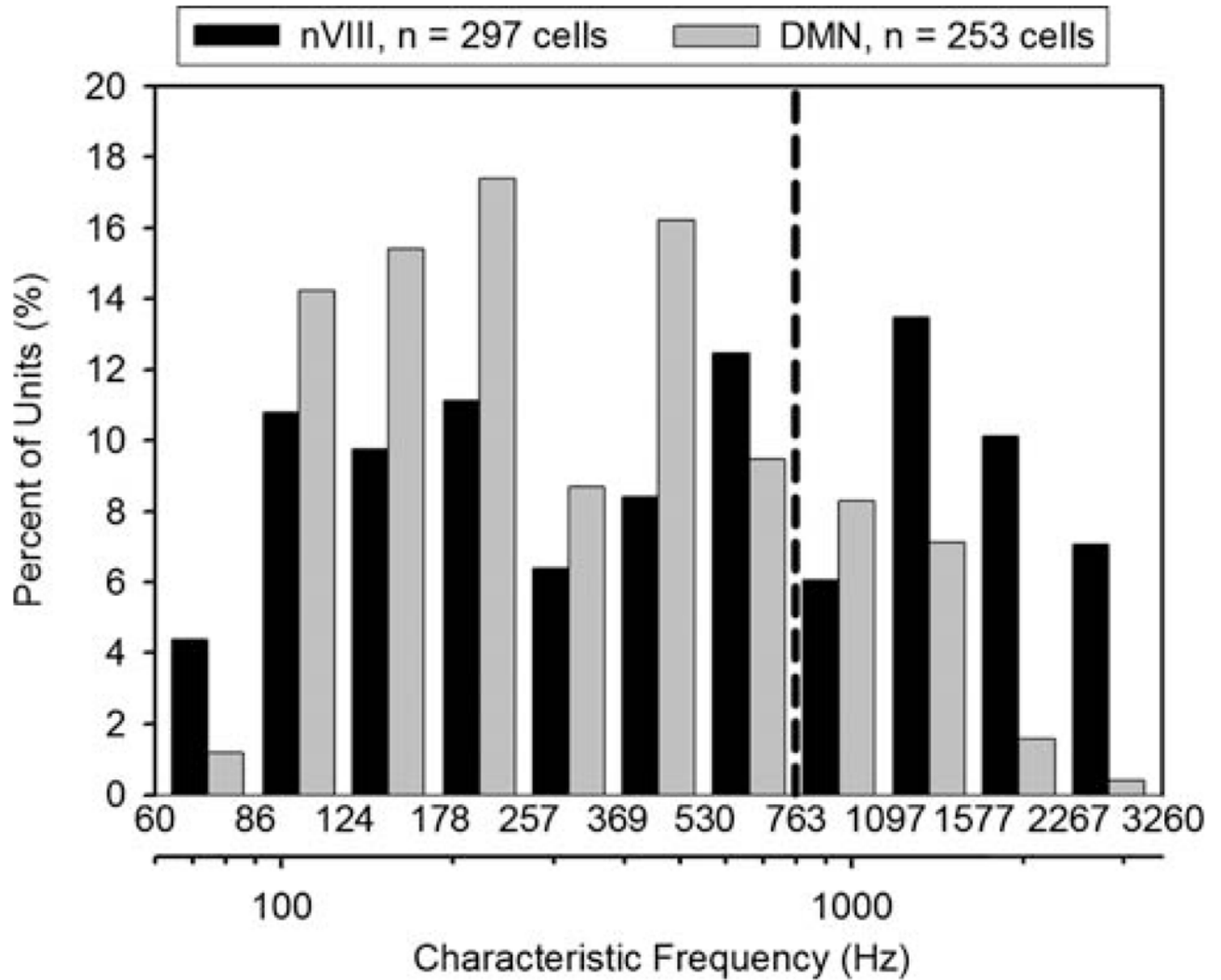
Fig. 4.
Logarithmic percentage histrogram of the CF distribution across 297 auditory nerve units
(*black bars*) and 253 DMN units (*gray bars*). CFs above 1 kHz probably belong to fibers
innervating the basilar papilla; fibers with CFs below 700 Hz most likely innervate the
amphibian papilla
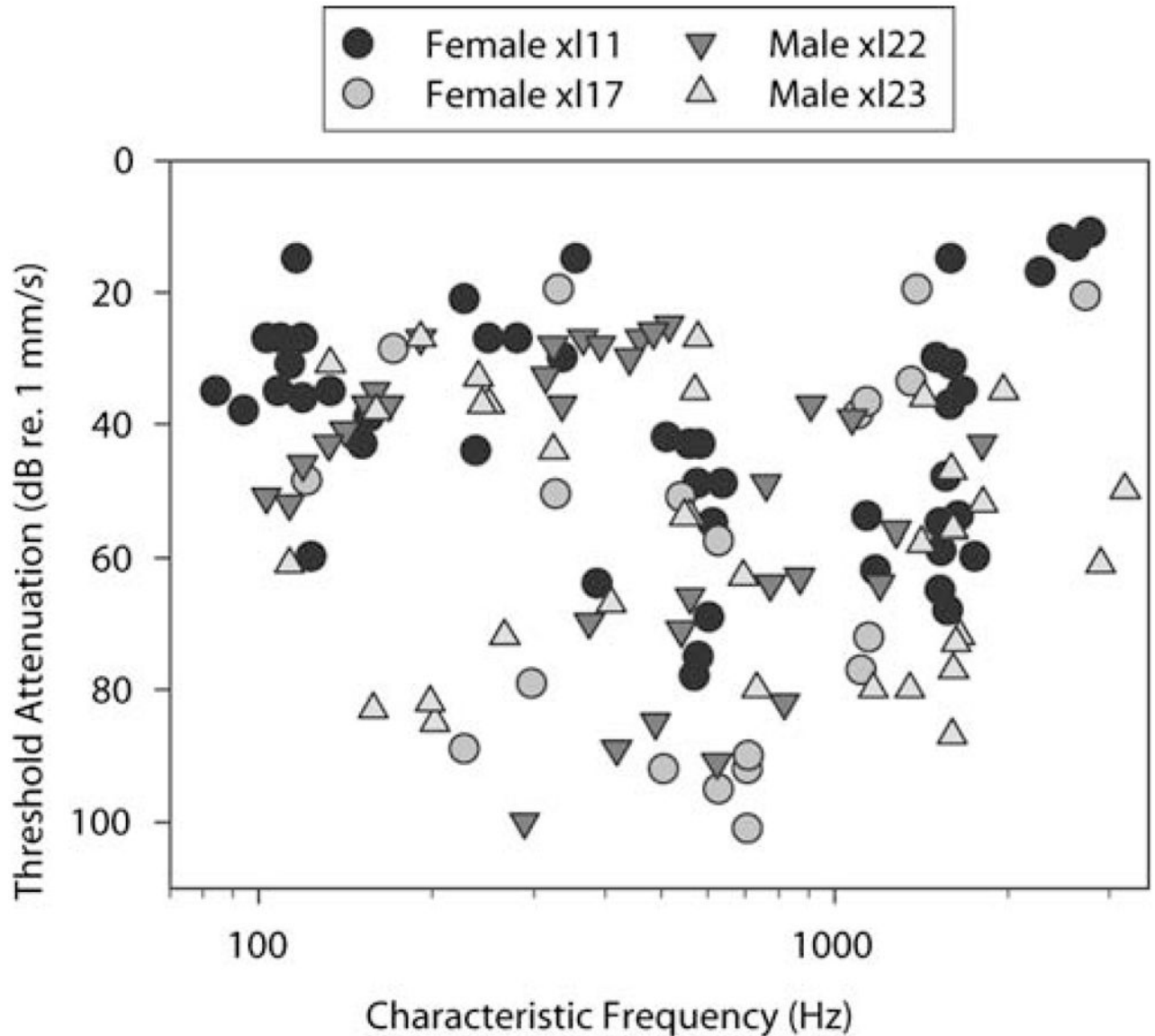
Fig. 5.
Thresholds taken at CF from FTCs in the 68 auditory nerve units recorded in two females (*circles*), and the 67 units recorded in two males (*triangles*). Minimum thresholds are similar at 250, 600 and 1,200 Hz. Two of the units with CFs above 2 kHz in the males are the only units in the whole population with thresholds below 40 dB attenuation re 1 mm/s in this range of frequency preference. In all other respects, male and female CF distributions and thresholds are similar
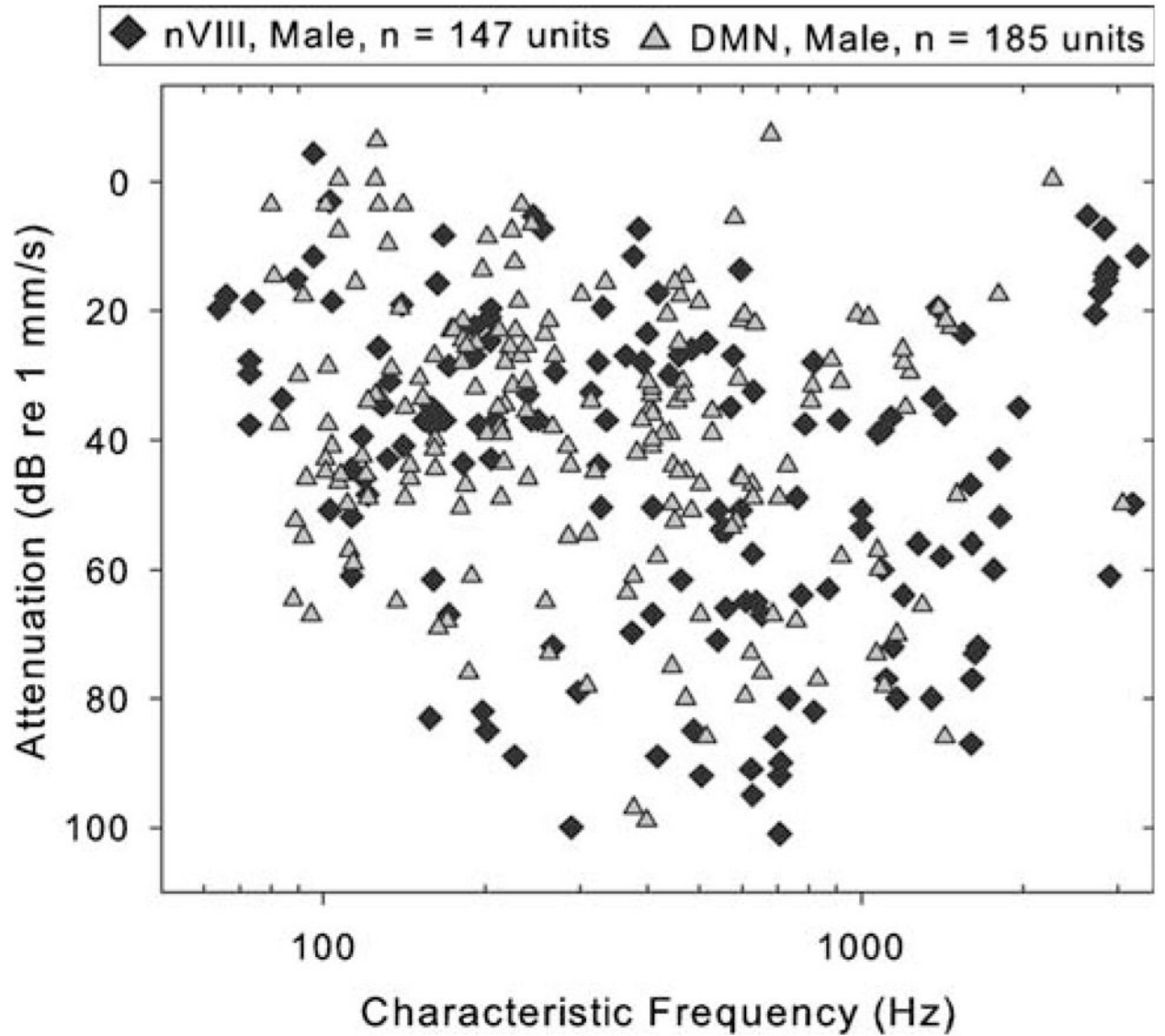
Fig. 6.
Sensitivity at CF threshold in nerve and DMN units recorded from all males. Relative to nerve recordings, the representation of high frequencies across the population of DMN recordings is less but thresholds are comparably sensitive. Male data is presented alone here because similar numbers of recordings were made in males but not females, facilitating comparison by the reader's visual inspection
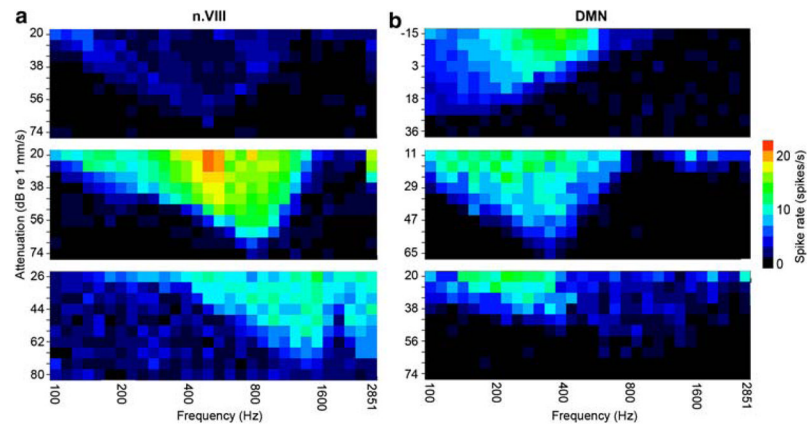
Fig. 7.

a Response area plots color-code the firing rate of three n.VIII fibers in response to 100-ms tone bursts at logarithmically spaced frequencies and level increments of 6 dB, presented in pseudorandom order along both axes. The three fibers differed in spontaneous activity, CF, and profile of sensitivity across frequency. The top nerve plot records an unusual cell that gave a non-monotonic rate-intensity curve, as reflected in its decreased firing at sound levels around 20 dB above the threshold edges of the response area. The bottom nerve plot represents an average of two experiments in a cell with inconsistent firing and a high spontaneous rate. **b** Response area plots, as in **a**, for three DMN cells. The unit at the top fired asymmetrically; at high sound levels, frequencies higher than CF elicited the fastest spike rates. The unit illustrated in the bottom graph had a "best frequency" (evoking the highest spike rate) much below CF
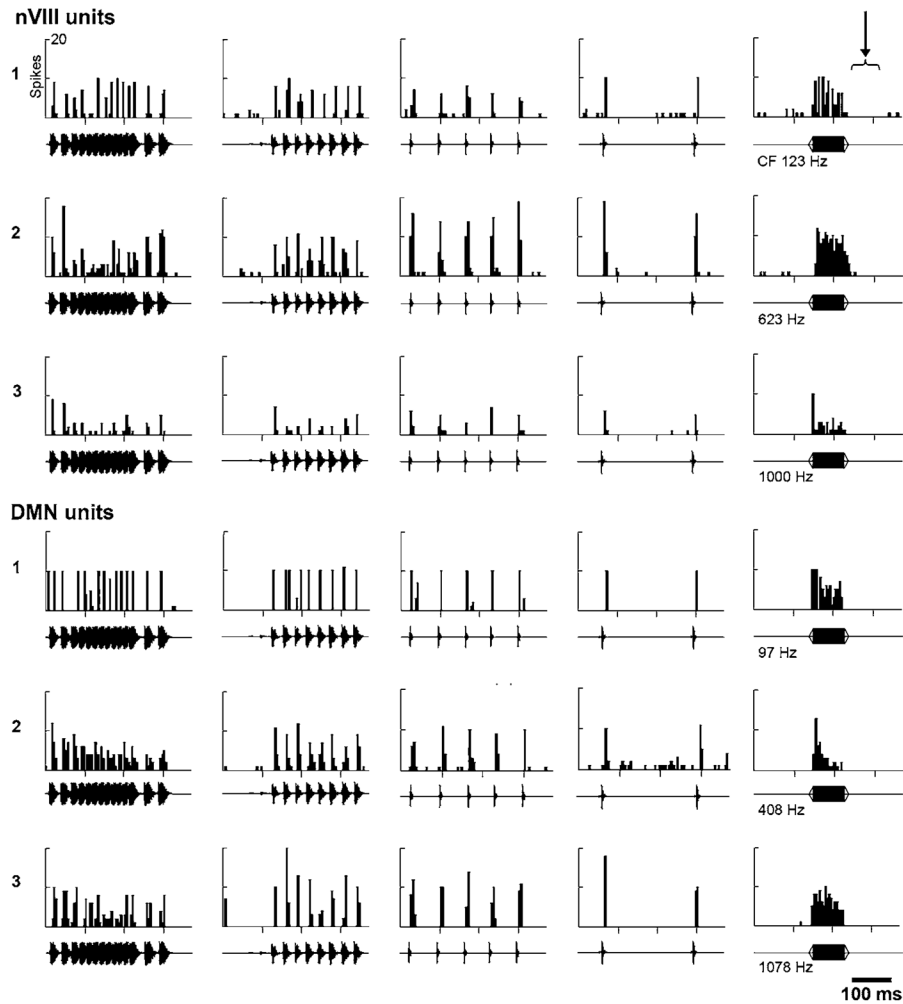
Fig. 8.
Post-stimulus time histograms (PSTHs) of responses to ten presentations of call stimuli (fast advertisement trill, slow advertisement trill, rapping and ticking, in order from left to right) and 100-ms pure-tone stimuli at CF in three n.VIII units and three DMN units. Units were selected to illustrate the population range in CF and temporal discharge patterns, but with moderately low spontaneous activity. Pure tone PSTHs (right-most column) are taken ~12 dB above threshold as determined by fitting cumulative normal distributions to rate-level functions. Call PSTHs are taken ~10 dB above the threshold estimated by visual inspection of responses to the suite of call stimuli. In low-frequency units (nVIII 1 and DMN 1), this level was about 35 dB above CF-tone threshold; in mid-frequency units (nVIII 2 and DMN 2) about 20 dB above threshold; and in high-frequency units (nVIII 3 and DMN 3) about 15 dB above threshold. Regardless of each unit's CF, spiking represents call envelopes, with temporal fidelity but without selection for click rate. Nerve units 1 and 2 and DMN unit 2 exhibited moderate spontaneous rates. In some units with spontaneous rates we noted post-stimulus suppression of activity (nVIII 1)
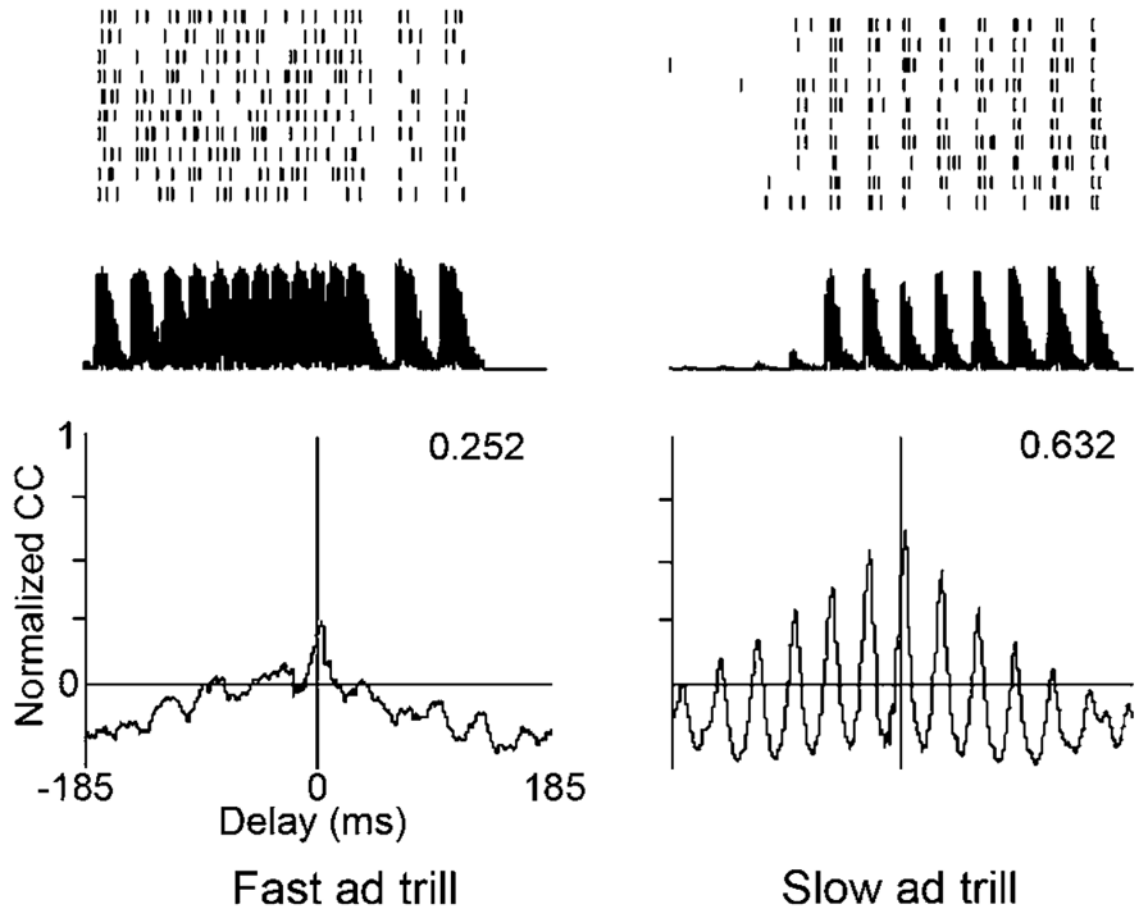
Fig. 9.
Spike trains in response to ten presentations of two natural call stimuli (*top*) and their cross-correlations (CC; *bottom*), taken from a nerve unit with a CF of 1,628 Hz. The PSTHs for the slow and fast advertisement trill 26 dB above CF threshold were cross-correlated with the stimulus envelopes shown below the spike rasters. The CC ordinate is scaled between 0 and the ideal cross-correlation for that PSTH (see "Materials and methods"). Delays at the peaks were 3.0 ms for the fast advertisement trill and 3.1 ms for the slow trill. Normalized CC peak values are shown in the upper right corner of the plots
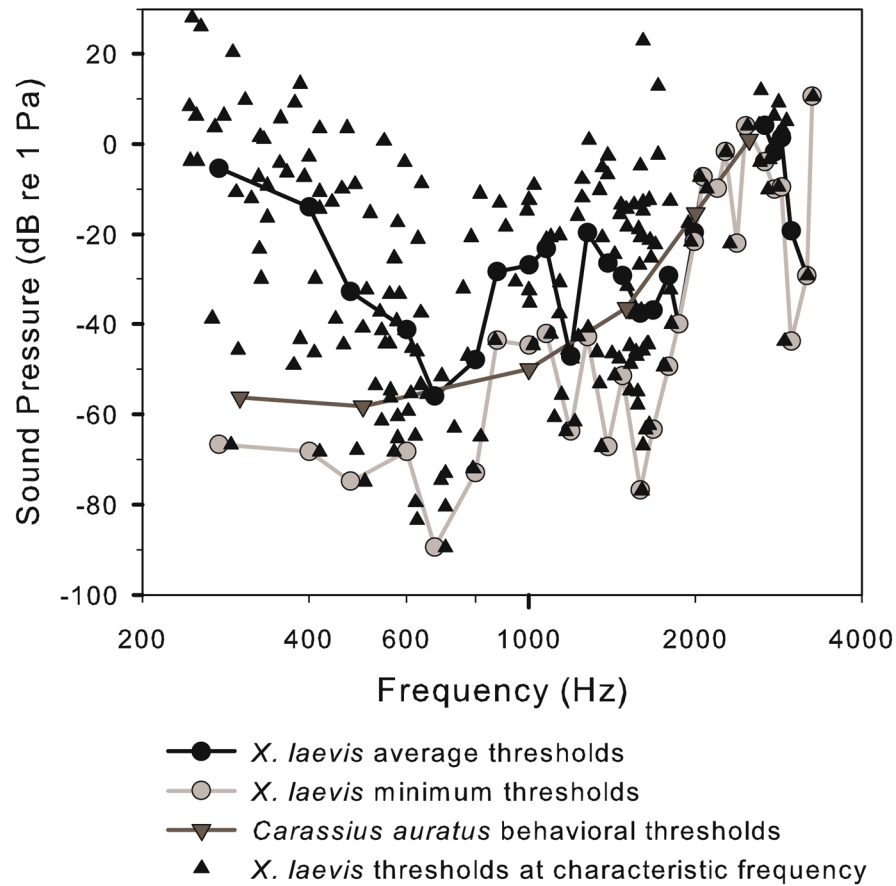
Fig. 10.
Average and mean thresholds in dB re 1 Pa, estimated from the population of CFs after transformation by tympanic vibration velocities measured by Christensen-Dalsgaard and Elepfandt (1995) to underwater 2 Pa tones over the range of 275–3500 Hz. Goldfish behavioral thresholds obtained using a shock avoidance paradigm are presented for comparison (Popper 1971). Frog minimum thresholds lie at 600 Hz and 1.6 kHz, with a tertiary peak at 3 kHz